Pathophysiology 26 (2019) 219–226

Contents lists available at ScienceDirect

Pathophysiology

journal homepage: www.elsevier.com/locate/pathophys

Cholesterol enriched diet suppresses ATF6 and PERK and upregulates the IRE1 pathways of the unfolded protein response in spontaneously hypertensive rats: Relevance to pathophysiology of atherosclerosis in the setting of hypertension

Lesya V. Tumanovska[a], R. James Swanson[b], Zoya O. Serebrovska[a,*], Georgii V. Portnichenko[a], Sergii V. Goncharov[a], Bohdan A. Kysilov[a], Olexandr O. Moibenko[a], Victor E. Dosenko[a]

[a] Department of General and Molecular Pathophysiology, Bogomoletz Institute of Physiology, Kyiv, Ukraine
[b] Liberty University College of Osteopathic Medicine, 306 Liberty View Lane, Lynchburg, VA 24502, USA

ARTICLE INFO

Article history:
Received 4 September 2018
Received in revised form 24 May 2019
Accepted 26 May 2019

Keywords:
Atherosclerosis
Cholesterol
UPR
SHR
CHOP
XBP1

ABSTRACT

Many studies have been dedicated to hypertension and hypercholesterolemia, as they are the primary conditions that influence the unfolded protein response (UPR). However, the concurrent effects of these two factors are unknown. Our research used spontaneously hypertensive rats (SHR) fed a cholesterol enriched diet (CED) as model of atherosclerosis formation to discover what effect the simultaneous actions of hypertension and hypercholesterolemia have on the UPR. The combination of hypertension and consumption of a CED (not the CED alone) caused the formation of early atherosclerotic features. Both increased expression of the CCAAT-enhancer-binding protein (CHOP) and the insulin induced gene 1 (INSIG1), which is the target gene of the sterol regulatory element-binding protein 1-c (SREBP1-c), and decreased expression of the spliced x-box binding protein1 (sXBP1) mRNA were observed in the SHR fed a CED. Cholesterol overload strongly suppressed glucose regulated protein 78 (GRP78), glucose regulated protein 94 (GRP 94), and the expression of CHOP and INSIG1 mRNA in both normotensive and hypertensive rats. Unlike other UPR factors, the sXBP1 mRNA expression was strongly downregulated in SHR fed a normal diet but upregulated in those fed a CED. The changes to UPR in the SHR fed a CED were associated with improvement of the initially impaired heart function of the rats.

1. Introduction

Atherosclerosis is the major underlying cause of cardiovascular disease and it is one of the leading causes of mortality and illness in developed countries [1]. The endoplasmic reticulum (ER) is the specialized perinuclear organelle where lipids, secretory molecules, and membrane proteins are synthesized. Thus, the ER is closely involved with the pathogenesis of atherosclerosis. The ER contains the lowest level of cholesterol and the high-affinity cholesterol sensors that reside there are responsible for cholesterol synthesis [2]. Cholesterol overload causes severe dysregulation of the ER [3].

The unfolded protein response (UPR) is an important adaptive mechanism that stabilizes ER function under conditions of accumulated misfolded proteins or other ER disturbances. In mammals, the UPR can be mediated by three ER unfolded protein receptors: ATF6, IRE1, and PERK [4,5].

Hypertension and increased blood cholesterol levels are the primary conditions responsible for atherosclerotic formations [6,7]. Hypertension causes activation of a UPR in rats [8–11]. According to the majority of publications, cholesterol overload leads to enhanced expression of GRP78, GRP 94, XBP1, CHOP, and other UPR components in yeast [12], in mouse macrophages [13,14], and in the isolated SMC [15] in rabbits [16] and in humans [17].

Initially, it was thought that the unique purpose of the UPR was to provide protein synthesis. However, it is now clear that the UPR is also closely related to lipid metabolism, particularly with the sterol regulatory element-binding proteins (SREBP), which have been shown to be the master regulators of both fatty acid and

* Corresponding author.
E-mail addresses: belyak-serebrovska@hotmail.com, dosenko@biph.kiev.ua (Z.O. Serebrovska).

https://doi.org/10.1016/j.pathophys.2019.05.005
0928-4680/

cholesterol metabolism [18]. Stress of the ER can activate the SREBP, through both the conventional site 1 and site 2 protease (S1P/S2P) proteolytic pathways and the caspases [19]. The XBP1s directly regulate the lipogenic genes in the liver [20]. The same proteases, S1p and S2p, ensure the processing of SREBP and ATF6 [21,22]. In turn, the SREBP affect the UPR. SREBP-1 binds directly to the regulatory regions of the genes encoding the ER stress signaling proteins, including the IRE1 [23].

Unlike other rats, the SHR demonstrate a low level of SREBP1 and SREBP2 expression as a result of the decreased activity of the promoter. This makes the SHR more sensitive to a dietary overload of lipids or carbohydrates [24,25].

We chose the SHR fed on a CED to study the combined effects of hypertension and hypercholesterolemia on the UPR. To characterize the three branches of the UPR, we examined the mRNA expression of GRP78, GRP 94, CHOP, and XBP1, as the target genes of ATF6, PERK, and IRE1, respectively, as well as the expression of INSIG1, which is the target gene of SREBP1-c. We found that consumption of a CED by the SHR caused formation of early atherosclerotic markers. Vigorous suppression of the UPR occurred in both the normotensive and the hypertensive rats fed a CED. Unlike the other UPR factors, the expression of XBP1 mRNA was strongly downregulated in the SHR fed a normal diet but upregulated in the SHR fed a CED.

2. Material & methods

The study protocol was approved by the Animal Care Ethics Committee of the Bogomoletz Institute of Physiology, Kyiv, Ukraine. The Wistar rats and the SHR were maintained in the animal quarters on a 12:12 h light/dark cycle at 22 ± 3 °C with food and water available ad libitum.

2.1. Study design

Sixteen 6-month-old male Wistar rats, weighting 294 ± 22 g, and sixteen 6-month-old male SHR, weighting 293 ± 43 g, were randomly divided into four groups of 8 rats each: Wistar Control, Wistar + CED, SHR Control, and SHR + CED. At the beginning of the experiment, all of the SHR rats were tested to verify their hypertensive status (arterial systolic pressure over 150 mmHg) using a Sphygmomanometer S-2 (HSE, Germany). For 8 weeks, the Wistar Control and SHR Control groups were fed standard rodent chow, while the Wistar + CED and SHR + CED groups were fed standard rodent chow enriched with 3% cholesterol. At the end of the experiment, all of the animals were anesthetized with urethane (1.5 g/kg) to allow measurement of the heart function, after which the rats were euthanized. The hearts were then extirpated and blood and aortic samples collected.

2.2. Cardio-hemodynamic parameters

A pressure-sensible micro-catheter 2 F (Millar Instruments, Houston, TX, USA) was injected retrograde into the left ventricles through a surgical cut-down of the right common carotid arteries [26]. Millar Instruments Software was used to perform the recording and the analysis of the basic cardio-hemodynamic parameters: i.e., heart rate, end-systolic pressure, end-diastolic pressure, end-systolic volume of the left ventricle, stroke volume, cardiac output, and others. The pressure and the volume ratios in the left ventricle were analyzed using the PVAN 3.6 program (Millar Instruments), with a conversion of the relative volume units (RVU) to absolute units of volume (μL) using the formula 'slope 20.25 X RVU -intercept 29.05.' For this purpose, the catheters were calibrated using the standard volume.

2.3. Lipid profile

The plasma cholesterol (Chol), triglycerides (TG), high density (HDL), low density (LDL), and the very low density lipoproteins (vLDL) were all measured using a Bio System A25 (Bio-Systems S.A., Spain). The atherogenic coefficients were calculated as (Total cholesterol – HDL cholesterol)/HDL cholesterol [27].

2.4. Morphological analysis

The heart-weight index was calculated as the relationship of the heart weight (mg) to the body weight (g). The lipid infiltration of the aortic wall was assayed using Oil Red (Sigma-Aldrich, USA). Slices of the frozen aortic arch (10–12 μm) were taken from three segments at intervals of 3–4 mm. The slices were then fixed on glass. A stock solution of Oil Red was diluted with isopropanol in a 3:2 ratio, filtered, and the micro samples stained for 10 min. The samples were then washed, stained with hematoxylin and eosin, and the morphological characteristics evaluated using a light microscope (Scope: Nikon, Eclipse E-200; Camera: Nikon, ds-FI1) at 200x, 400x, and 1,000 ×.

For the electron microscopic study, the aortic wall slices were fixed in 2% paraformaldehyde with 2.5% glutaraldehyde in a 0.1 M phosphate buffer (pH 7.4) for 2 h and then post-fixed in 1% buffered osmium tetroxide. After dehydration in graded ethanol, tissues were embedded in epoxy resin (Fluka). The ultrathin sections, double stained with uranyl acetate and lead citrate, were examined with an electron microscope (Jem-100CX; Jeol, Japan).

2.5. RNA isolation, reverse transcription, and the real-time polymerase chain reaction

The total RNA was isolated from the aorta and heart tissue using a TRIzol RNA-Prep Kit (Isogen, Russian Federation) following the manufacturer's protocol. The RNA concentration was determined using a NanoDrop Spectrophotometer ND1000 (NanoDrop Technologies Inc., USA). The reverse transcription was performed using a RevertAid™ H Minus First Strand cDNA Synthesis Kit (Fermentas, Germany), on 1.2–1.5 μg of the total RNA with a random hexamer primer. The single-stranded DNA obtained was used for the real-time polymerase chain reaction (PCR).

2.6. Real-time PCR for analysis of the mRNA expression of the GRP78, GRP94, sXBP1, uXBP1, CHOP, and INSIG1 genes

The amplification was performed in 10 μL of SYBR Green PCR Master Mix containing 20 pM of each primer. For the amplification of the GRP78, GRP94, sXBP1, uXBP1, CHOP, INSIG1, and ACTB (corresponding to b-Actin, the housekeeping gene) gene fragments, the following primers (Table 1) were used, respectively.

The sample volume was brought up to 20 μL with deionized water. The amplification was performed on a 7500 Fast Real-Time PCR System. The amplification program consisted of an initial AmpliTaq® Gold DNA polymerase activation step at 95 °C for 10 min followed by 50 cycles: denaturation (95 °C for 15 s) and then annealing and elongation (56 °C for 60 s). For the control of the specificity, a dissociation stage sequential increase of temperature from 56 °C to 99 °C was performed. The drop in the double-stranded DNA-SYBR Green complex fluorescence strength was recorded. The calculation was performed using 7500 Fast System SDS Software. The cycle threshold was defined as the number of cycles required for the fluorescence signal to exceed the detection threshold. The expression of the target gene relative to the housekeeping gene was calculated as the difference between the threshold values of the two genes.

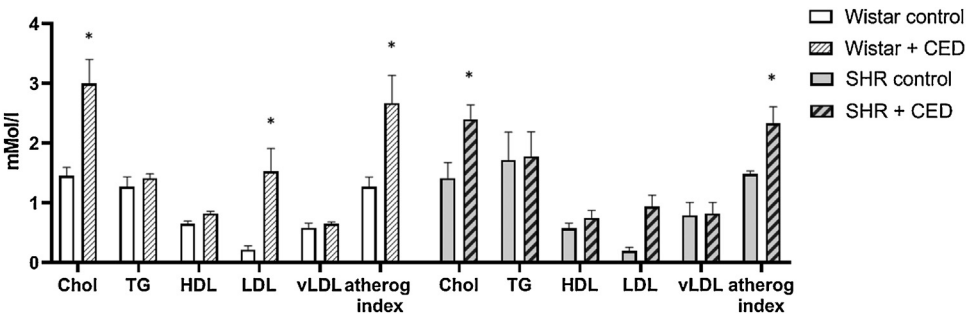

Fig. 1. Plasma lipids. Values are means±SE *$P < 0.05$ compared to Wistar control; #$P < 0.05$ compared to SHR control.

Table 1
Primer sequences for determination of β-actin, GRP78, GRP94, sXBP1, uXBP1, and CHOP levels.

Target gene	Primer sequence	PCR product size (bp)
β-actin	5'-AAGTCCCTCACCCTCCCAAAAG-3' 5'-AAGCAATGCTGTCACCTTCCC-3'	97
GRP78	5'-ACCATGGAGAAAGCTGTAGAGG-3' 5'-GCCTCCACTTCCATAGAGTTTG-3'	142
GRP94	5'-TGACCAGAGAGGAGCTGGTTA-3' 5'-CCGTCTTCTTGTGCTTCTGTC-3'	95
sXBP1	5'-GCTTGTGATTGAGAACCAGG-3' 5'-GGCCTGCACCTGCTGCGGACTC-3'	141
uXBP1	5'-ACACGCTTGGGGATGAATGC-3' 5'-CCATGGGAAGATGTTCTGGG-3'	159
CHOP	5'-CTTCACTACTCTTGACCCTGCAT-3' 5'-CCGTTTCCTAGTTCTTCCTTGAT-3'	161
INSIG1	5'-GTGGGAAACATAGGACGACAGT-3' 5'CAGTGTCTCCACATTCTGCTTC-3'	90

2.7. Statistics

All of the values are presented as an arithmetic mean ± standard error. The analyses of variance were performed using one-way ANOVA, together with a post-hoc analysis when using the Bonferroni correction. The results were considered statistically significant when $P < 0.05$. The software used was MS Excel 2010 and Origin Pro 8.5.

Funding statement

This study was funded by the National Academy of Sciences of Ukraine.

3. Results

3.1. Plasma lipid profile

The levels of total cholesterol and LDL-cholesterol, as well as the atherogenic index, were increased in both the normotensive (Wistar + CED) and the hypertensive (SHR + CED) rats fed a CED. The plasma TG, HDL, and vLDL levels did not differ from those of the control groups (Fig. 1).

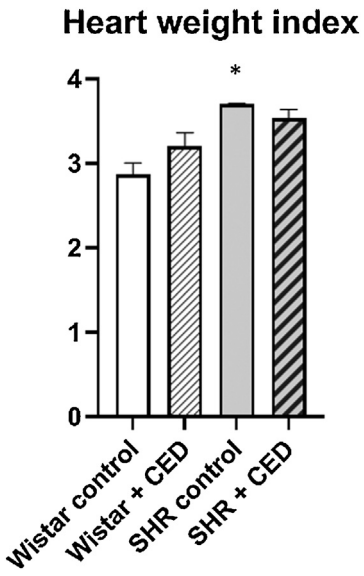

Fig. 2. Heart weight index of Wistar and SHR rats fed either a standard diet or a CED. *$P < 0.05$ compared to Wistar Control.

3.2. Heart function and morphology

Significant irregularities of the heart function parameters in the SHR control group were observed. The cardiac output was decreased 3.5-fold due to decreased heart rate and stroke volume. The maximum blood pressure increased (Table 2) and the myocardium was hypertrophied (Fig. 2).

The heart function was impaired in the normotensive rats fed the CED (Wistar + CED group); the cardiac output decreased due to reduced heart rate and stroke volume. The maximum pressure decreased. The relative myocardial mass did not change.

Unlike the normotensive rats, the hypertensive rats (SHR + CED group) showed improvement in their heart function when fed the CED; the cardiac output was enhanced due to increased stroke volume and the maximal pressure decreased down to the levels of the Wistar Control group.

Table 2
Heart function parameters. *$P < 0.05$ compared to Wistar Control; #$P < 0.05$ compared to SHR Control; &$P < 0.05$ compared to Wistar+CED.

	Wistar	SHR	Wistar + CED	SHR + CED
End-systolic Pressure (mmHg)	95.42 ± 0.68	110.98 ± 0.42*	128.22 ± 2.25*#	111.12 ± 4.99
End-diastolic Pressure (mmHg)	1.36 ± 0.24	5.72 ± 0.38*	2.64 ± 0.25*#	5.29 ± 0.63*
Stroke Volume (μL)	254.40 ± 4.30	77.22 ± 2.75*	201.51 ± 7.62*#	114.67 ± 15.29*#
Ejection Fraction (%)	34.8 ± 0.36	15.10 ± 0.40*	35.26 ± 0.66#	17.81 ± 1.44*
Cardiac Output (μL/min)	93,337 ± 1760	23698 ± 856*	62,423 ± 2130*#	34,978.5 ± 5760.0*
Arterial Elastance (Ea) (mmHg/μL)	0.413 ± 0.006	2.01 ± 0.06*	0.96 ± 0.03*#	1.997 ± 0.35*
Tau_w (ms)	7.81 ± 0.06	10.08 ± 0.14*	9.64 ± 0.21*	10.7 ± 0.35*

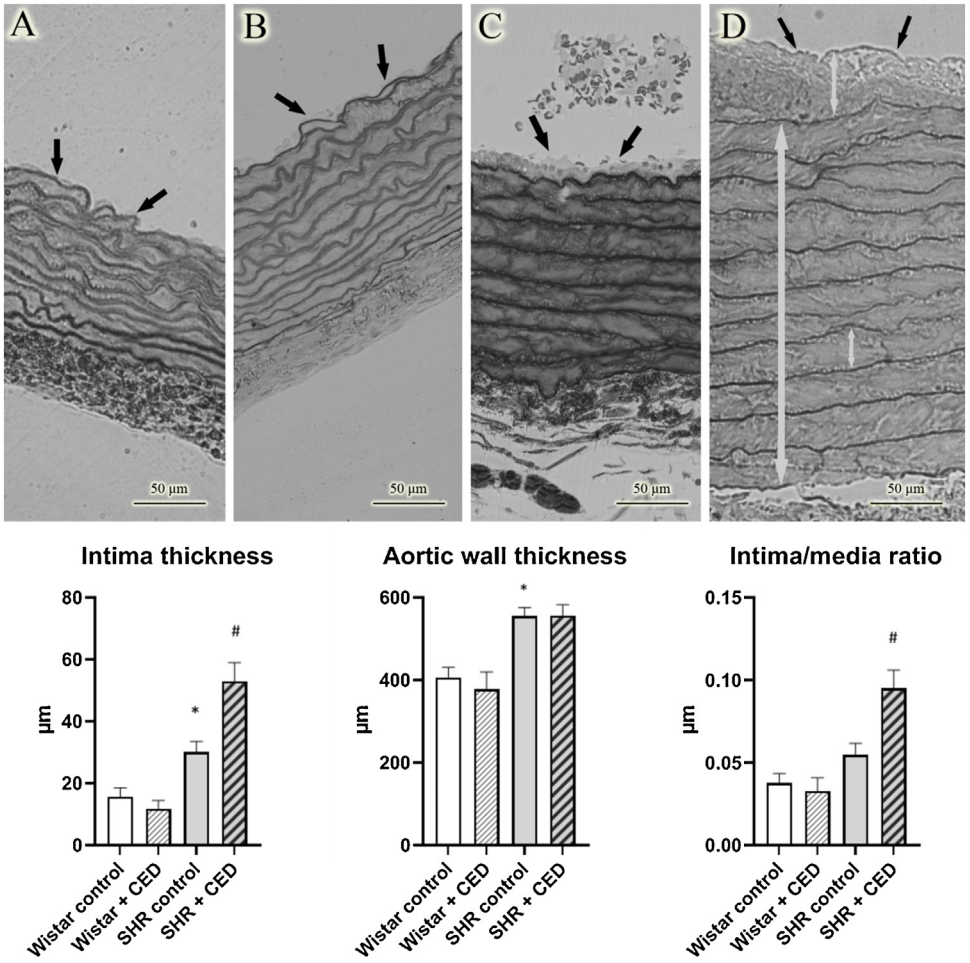

Fig. 3. Semi-thin sections of aortic wall: A, Wistar + CED; B, SHR control group; C & D, SHR + CED. White arrows indicate the thickness of the intima, media, and one SMC layer; black arrows indicate the intima in different experimental groups. E, Intima, aortic wall thickness, and intima/media ratio of different groups. *$P < 0.05$ compared to Wistar Control; #$P < 0.05$ compared to SHR Control.

3.3. Aortic wall characteristics

Unlike observations in the SHR Control and SHR + CED groups, mild changes were seen in the aortic wall of the normotensive rats after consumption of the CED (Wistar + CED group). Local sub-endothelial layer vacuolization with partial endothelium desquamation and detachment occurred. No pronounced morphological alterations were observed (Fig. 3B). No differences arose in the aortic wall, tunica intima thickness, intima/media ratio (Fig. 3), tunica media thickness, or in the number of the SMC layer (data not shown).

Chronic hypertension caused pronounced changes in the aortic wall (SHR Control group). The tunica media thickness and the number of the smooth muscle layer did not differ from that of Wistar Control group (data not shown), but the tunica intimae and the aortic wall thicknesses, as well as the intima-media ratio, were significantly greater than in the Wistar Control group (Fig. 3E). Significant changes in the various vascular wall layers were observed: i.e., endothelial thinning, endothelial desquamations, edema of the tunica intimae, and fragmentation of the internal elastic laminae (Fig. 3).

The electron microscopic study confirmed a number of ultrastructural changes in the different layers. In particular, we observed thickening of the tunica intimae, which occurred due to edema and fragmentation of the internal elastic laminae, and disarrangement of the endothelial layers, with significant endothelial cells thinning, endothelium desquamation, complete internal elastic laminae denudation, cell shape alteration, and expansion of the inter-endothelial junctions (Fig. 4).

Some inter-endothelial junctions were less dense and some areas demonstrated a spatial reorientation of the SMC relative to the endothelial layers (Fig. 4B). There were a number of intracellular disorders: the majority of the mitochondria were edemic, with partially or completely destroyed cristae. We observed numerous vacuoles of different origins, including autophagies (Fig. 4C).

The combination of hypercholesterolemia with hypertension (SHR + CED group) led to more pronounced morphologic disorders. The tunica intimae thickness and the intima-media ratio were significantly higher than in the SHR Control group (Fig. 3). As in the SHR Control group, endothelial thinning, endothelial desquamation, complete internal elastic laminae denudation, edema of the intimae, and fragmentation of the internal elastic laminae were observed in the aortic wall of the SHR + CED rats; however, the areas of change were much larger in this group (Fig. 4D, E, and F). The SMC migrated into the sub-endothelial layers (Fig. 4F). ER edema occurred in the endotheliocytes, as well as in the SMC of the SHR + CED group (Fig. 5), but this was not observed in the SHR control group. ER edema was a feature of the developing ER stress [28,29].

Lipid infiltration was not observed in the Wistar + CED group, but it was observed to a minor extent in the SHR control group, as well as in the SHR + CED group (up to 2.79%; Fig. 6). The totality of these features in the SHR + CED group may indicate the initial stages in the formation of atherosclerosis.

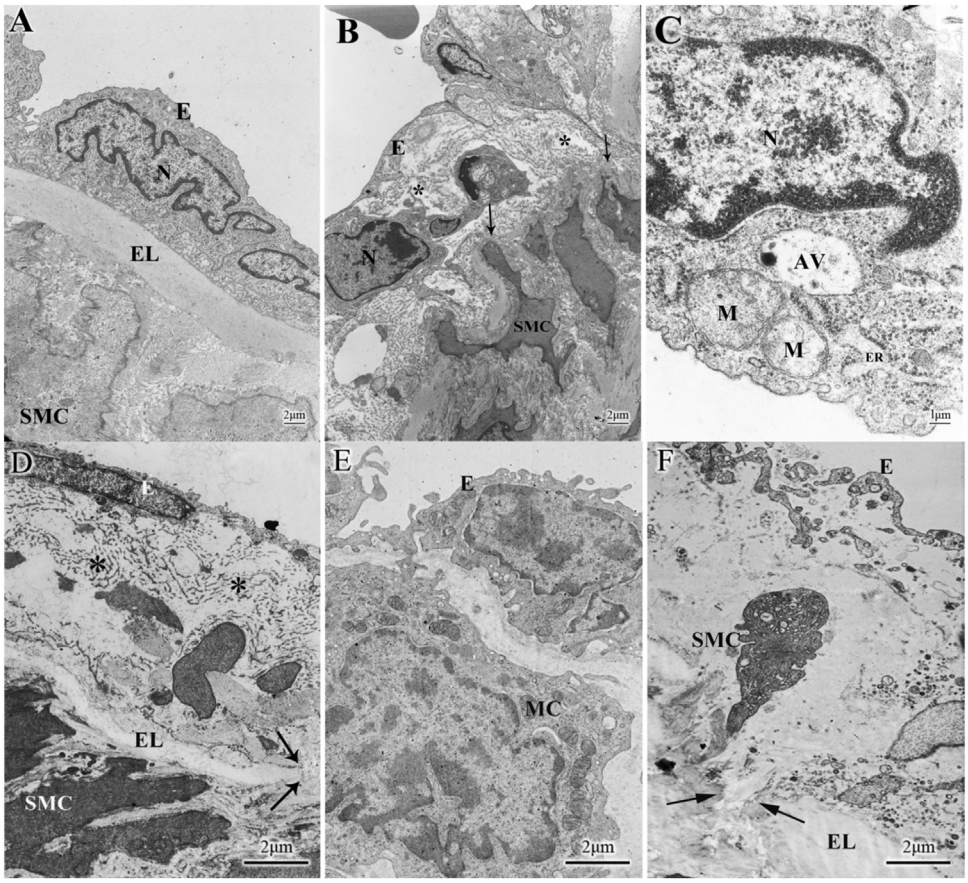

Fig. 4. Ultrastructural changes in rat aortas. A, Wistar Control. Micrograph show a distinct organization of endothelial and SMC layers, separated by elastic laminae with typical width. B, SHR Control. In the SHR aorta, evidence of endothelial and SMC disorganization was identified. Osmiophilic nuclei of endotheliocytes often appeared to have a different spatial orientation. Sub-endothelial edema (*) contributed to endothelial desquamation. Elastic laminae fragmentation (↑) and disorganization of SMC with finger-like projections of cytoplasm were displayed. C, The segment of the endothelial cells cytoplasm containing autophagic vacuoles and dilated ER (↑). D, SMC localized in the sub-endothelial space and surrounded by collagen matrix (*). E, Monocytes localized in the sub-endothelial space. F, SMC with vacuolated cytoplasm migrated into the intima. Endothelial thinning with intercellular junction disruption and fragmentation of elastic laminae (↑) in aortic specimens.

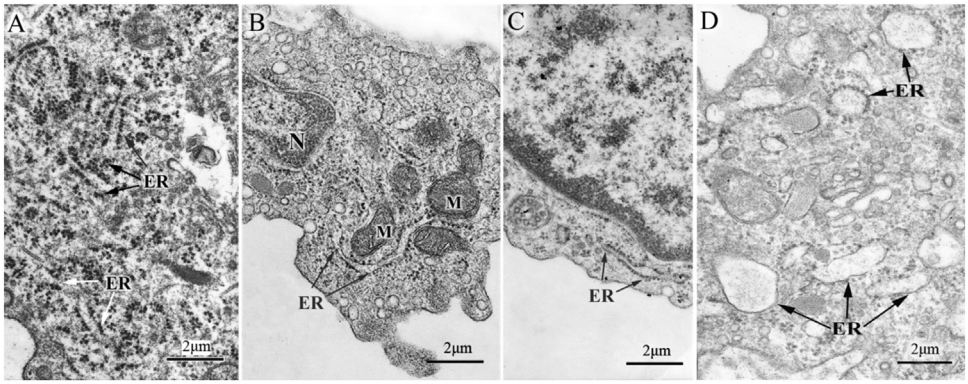

Fig. 5. Structure of aortal endotheliocytes. The photographs show that in the Wistar Control (A), Wistar + CED (B), and SHR Control (C) groups the ER cisterns are not expanded and retain their structure. The significant dilation of the ER lumen was displayed (↑), indicating development of stress in the ER in SHR + CED (D). Abbreviations: E, endotheliocyte; ER, endoplasmic reticulum; M, mitochondria, N, endothelial cells nucleus.

3.4. Expression of the INSIG1 and UPR factors

The INSIG1 expression was higher in the SHR compared to the Wistar rats who consumed a normal diet and it was downregulated in those who consumed a CED. No differences in the INSIG1 expression were observed in the Wistar rats who consumed the CED (Fig. 7).

The GRP78 expression in the aorta of the Wistar control rats was 5x higher than in the heart tissue. No significant difference was observed between GRP78 expression in the controls and the SHR. Consumption of the CED caused a remarkable downregulation of the GRP78 mRNA expression in both the normotensive (72x aorta; 4.9x heart (Wistar + CED group)) and the hypertensive (65x aorta and 7x heart (SHR + CED)) rats. The GRP94 expression in the aorta of the Wistar control rats was 2.5-fold higher than that in the heart tissue.

No significant enhancement of the GRP94 expression occurred in either the aorta (3x) or the heart (5x) of the SHR Control group.

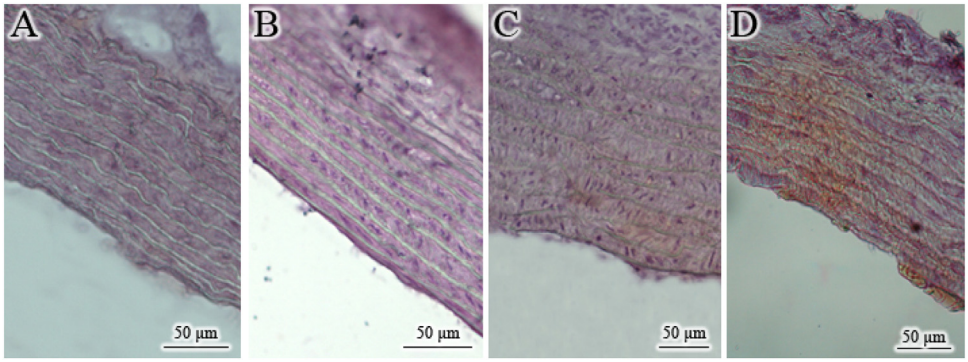

Fig. 6. Images of Wistar and SHR rat aortic wall samples; Oil Red staining indicates lipid infiltration. A, aortic wall of Wistar Control rats (no lipid infiltration); B, aortic wall of Wistar + CED rats; C, aortic wall of SHR Control rats (slight lipid infiltration); D, aortic wall of SHR + CED rats (considerable lipid infiltration) (For interpretation of the references to colour in this figure legend, the reader is referred to the web version of this article).

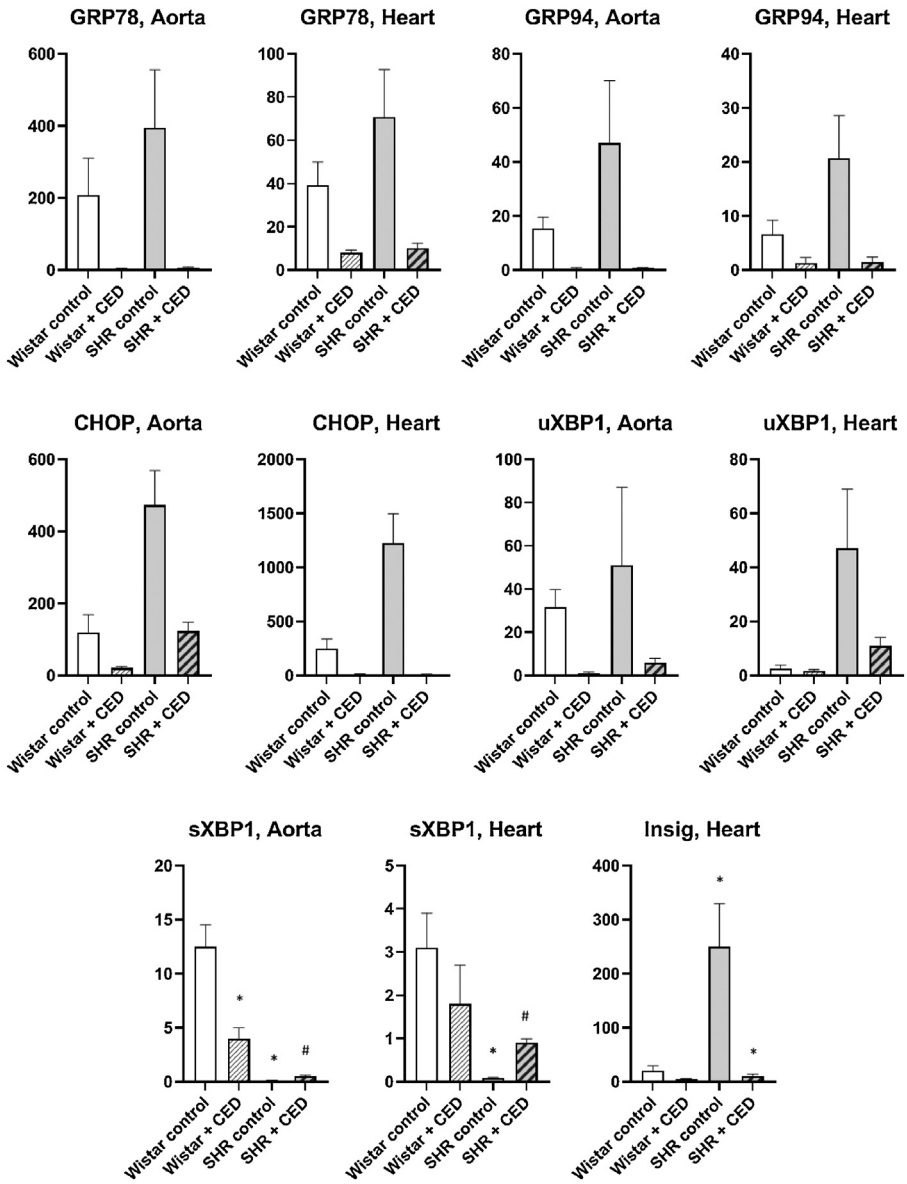

Fig. 7. Expression of mRNA INSIG1 in heart and expression of mRNA GPR78, GRP94, CHOP, uXBP, and sXBP1 in aorta and heart of different groups.*$P < 0.05$ compared to Wistar Control; #$P < 0.05$ compared to SHR Control.

The GRP94 mRNA expression was significantly downregulated in the CED-fed normotensive rats (30.8x aorta; 4.9x heart (Wistar + CED group)) and the CED-fed hypertensive rats (67x aorta; 13.8x heart (SHR + CED group)). The CHOP expression in the aorta of the Wistar control rats was 2-fold less than that in the heart tissue.

We observed a significant increase in the CHOP expression (3.9x aorta; 5x heart) in the SHR Control group. Consumption of the CED caused a significant downregulation of the CHOP mRNA expression in both the normotensive and the hypertensive rats (Wistar + CED group and the SHR + CED group). The repression of the CHOP expression was exceptional in the heart: 250-fold for the normotensive rats; 1220-fold for the hypertensive rats. The uXBP1 expression in the aorta of the Wistar control rats was 12-fold higher than in the heart.

No significant changes occurred in the uXBP1 expression in the SHR control group. Consumption of the CED caused no significant change in uXBP1 mRNA expression in the heart of the normotensive rats or the hypertensive rats, but a 30-fold decrease in the expression of uXBP1 mRNA was seen in the aorta of the normotensive rats. The sXBP1 expression in the heart was very low.

There was a significant downregulation of the sXBP1 expression (140x in the aorta and 34x in the heart). Consumption of the CED caused significant downregulation of the expression of sXBP1 mRNA in the normotensive rats (Wistar + CED group) and an upregulation in the hypertensive rats (SHR + CED group), in both the aorta and the heart.

4. Discussion

The UPR is a normal physiological reaction used by cells to prevent an accumulation of unfolded and misfolded proteins in the ER, as well as to improve the normal ER function. Under pathologic conditions, such as hypertension, the ER function becomes impaired, leading to the development of ER stress; long-term hypertension has been shown to be an effective stimulus for ER stress progression [30]. In this study, we observed similar adaptive effects of the UPR factors to hypertension. There were no significant enhancements of the expression of either GRP94 or GRP78 in both the aorta and the heart of the SHR Control group. The upregulation of the INSIG1 expression, which is a target of SREBP1-c, is consistent with the CHOP activation in the SHR [20]. Unlike the other UPR factors, the sXBP1 mRNA expression was strongly downregulated in the SHR. Thus, we observed activation of ATF6 and PERK and repression of the IRE1 pathways for the UPR in the SHR consuming a normal diet. Stress to the ER caused cleavage of uXBP1 pre-mRNA, which produced a mature sXBP1 mRNA in its activated form, a process exclusively regulated by the IRE1 [31]. In these experiments, the lack of sXBP1 mRNA in the aorta and the heart of the SHR control rats was accompanied by an unchanged uXBP1 mRNA expression, suggesting an inactivation of the IRE1 endoribonucleolytic activities. The product of an sXBP translation regulates a subset of the UPR genes that promote the ER-associated degradation (ERAD) of the misfolded proteins [32]. Thus, such an inactivation of the IRE1 pathway probably aggravated the stress on the ER and increased the risk of cell death. The study of Jonathan H. et al. demonstrated an attenuation of the IRE1 and a strong diminution of sXBP1 mRNA expression levels under persistent ER stress in cell cultures, which negatively affected the cell survival [33]. Chronic hypertension caused prolonged ER stress and also led to a suppression of the IRE1 pathway.

The effect caused by consumption of the CED on the UPR was unexpected. Unlike the many studies in the literature that have shown UPR activation in response to consumption of a high fat diet, in this study, a cholesterol overload caused a powerful suppression of the expression of GRP78, GRP94, CHOP, and uXBP1 mRNA, in both the normotensive and the hypertensive rats. Moreover, the sXBP1 mRNA expression, which was strongly downregulated in the SHR group who consumed a normal diet, became upregulated in response to consumption of the CED.

The peculiarities of a rat's metabolism may possibly explain such a discrepancy. Data in the literature show that a cholesterol overload has caused UPR activation in other biological species, but not in rats. Only a few studies exist that have been dedicated to studying UPR after CED consumption in rats. Ahmed et al. showed no differences in the expression of GRP78, CHOP, or XBP1 in the liver of Sprague-Dawley rats after 5 weeks of consumption of a high fat diet [30]. Another study showed no differences in the expression of GRP78 or CHOP in the heart tissue of Wistar rats fed 1.5% cholesterol in their lab chow, with the addition of other cholesterol enriched products, for 8 weeks [31]. The same discrepancy was observed when we examined the vessel morphology. The alterations in the aortic wall that occurred under cholesterol overload were not the main atherosclerotic features that might have been expected. Unlike rabbits, hamsters, guinea pigs, and other herbivores, who easily develop atherosclerotic lesions when consuming a cholesterol enriched diet [34], rats are much more resistant to atherogenesis, which could be attributed to the high HDL content of their blood [35].

Nevertheless, the results of this research raise questions about the pathophysiological roles of the downregulation of GRP78, GRP94, CHOP, and uXBP1 expression and the activation of sXBP1 in response to the consumption of a CED in rats. One possible mechanism may be connected to the protective action of the bile acids, the circulating levels of which are enhanced under a cholesterol overload. In a study by Choi et al., the UPR was downregulated in the SHR under the influence of tauroursodeoxycholic acid, which binds to the hydrophobic regions of the proteins and prevents protein aggregation [36].

XBP1 mRNA is a potent transcriptional activator. Splicing of the XBP-1 has previously been shown to initiate the transcription of the genes involved in protein folding, transport, and ER-associated protein degradation. Recent studies have provided evidence that the XBP1-mediated UPR plays a protective role under inflammatory conditions, such as those that occur in chronic kidney disease or retinal endothelial inflammation [37]. On the other hand, most GRP78 and IRE1 related mechanisms are known to prevent the progression of atherosclerosis in the early stages [38]. Thus, upregulation of sXBP1 under a cholesterol overload can be considered a protective mechanism.

A cholesterol overload suppressed the expression of SREBP1-c. On the one hand, this was to be expected as the result of downregulation of the lipid metabolism. On the other hand, this can partially explain the dynamics of the XBP1. Sanchez-Alvarez M et al. demonstrated that a sustained depletion of SREBP significantly increased the levels of XBP1 splicing in proliferating cells [39].

All of the abovementioned UPR reactions were accompanied by alterations in heart function and in the structure of the aorta. The prolonged hypertension tended to alter the vessel wall shape and its composition by changing the migration, proliferation, apoptosis of the endothelial cells, and the SMC, as well as the synthesis and the degradation of the extracellular matrix [40]. In this study, chronic hypertension led to damage in the aortic wall. The vascular damage was associated with a severe impairment of the pumping function of the heart, accompanied by hypertrophy.

The simultaneous actions of cholesterol overload and hypertension caused atherosclerotic features to form in the aortic walls. At the same time, the cholesterol overload caused improvements to heart function. These results concur with the data in the literature that support the cardioprotective action of a high fat diet against ischemia-reperfusion injury through the NF-κB-dependent regulation of the cell death pathways in the heart [38].

5. Conclusion

A cholesterol overload caused a powerful suppression of the expression of GRP78, GRP94, CHOP, and the INSIG1 mRNA in both normotensive and hypertensive rats. Unlike other facets of the UPR, the sXBP1 mRNA expression was upregulated in response to the consumption of a CED. These changes to the UPR in SHR who consumed a CED were associated with the early stages of atherosclerosis, as well as with improvement of the initially impaired heart function. The mechanisms of this specific action of cholesterol in rats needs much further research.

References

[1] J. Zhou, S. Lhoták, B.A. Hilditch, R.C. Austin, Activation of the unfolded protein response occurs at all stages of atherosclerotic lesion development in apolipoprotein E-deficient mice, Circulation 111 (April (14)) (2005) 1814–1821, Epub 2005 Apr 4.

[2] P.L. Faust, W.J. Kovacs, Cholesterol biosynthesis and ER stress in peroxisome deficiency, Biochimie 98 (March) (2014) 75–85.

[3] B. Feng, P.M. Yao, Y. Li, C.M. Devlin, D. Zhang, H.P. Harding, M. Sweeney, J.X. Rong, G. Kuriakose, E.A. Fisher, A.R. Marks, D. Ron, I. Tabas, The endoplasmic reticulum is the site of cholesterol-induced cytotoxicity in macrophages, Nat. Cell Biol. 5 (2003) 781–792.

[4] A. Chakrabarti, A.W. Chen, J.D. Varner, A review of the mammalian unfolded protein response, Biotechnol. Bioeng. 108 (December (12)) (2011) 2777–2793.

[5] A.X.1 Zhou, I. Tabas, The UPR in atherosclerosis, Semin. Immunopathol. 35 (May (3)) (2013) 321–332, http://dx.doi.org/10.1007/s00281-013-0372-x, Epub 2013 Apr 4.

[6] T.E. O'Toole, D.J. Conklin, A. Bhatnagar, Environmental risk factors for heart disease, Rev. Environ. Health 23 (Jul-Sep (3)) (2008) 167–202.

[7] M.J. van Rooy, E. Pretorius, Obesity, hypertension and hypercholesterolemia as risk factors for atherosclerosis leading to ischemic events, Curr. Med. Chem. 21 (19) (2014) 2121–2129.

[8] L. Liu, J. Liu, Z. Huang, X. Zhang, D. Dou, Y. Huang, Berberine improves endothelial function by inhibiting endoplasmic reticulum stress in the carotid arteries of spontaneously hypertensive rats, Biochem. Biophys. Res. Commun. 458 (March (4)) (2015) 796–801, http://dx.doi.org/10.1016/j.bbrc.2015.02.028, Epub 2015 Feb 14.

[9] S.K. Choi, M. Lim, S.H. Byeon, Y.H. Lee, Inhibition of endoplasmic reticulum stress improves coronary artery function in the spontaneously hypertensive rats, Sci. Rep. 6 (August) (2016) 31925.

[10] Y. Sun, T. Zhang, L. Li, J. Wang, Induction of apoptosis by hypertension via endoplasmic reticulum stress, Kidney Blood Press. Res. 40 (1) (2015) 41–51.

[11] Y. Ge, G. Li, B. Liu, H. Guo, D. Wang, Q. Jie, W. Che, L. Hou, Y. Wei, The protective effect of Lacidipine on myocardial remodeling is mediated by the suppression in expression of GPR78 and CHOP in rats, Evid. Complement. Alternat. Med. (2019).

[12] L. Pineau, T. Ferreira, Lipid-induced ER stress in yeast and β cells: parallel trails to a common fate, FEMS Yeast Res. 10 (December (8)) (2010) 1035–1045.

[13] S. Yao, C. Zong, Y. Zhang, H. Sang, M. Yang, P. Jiao, Y. Fang, N. Yang, G. Song, S. Qin, Activating transcription factor 6 mediates oxidized LDL-induced cholesterol accumulation and apoptosis in macrophages by up-regulating CHOP expression, J. Atheroscler. Thromb. 20 (1) (2013) 94–107.

[14] B. Feng, P.M. Yao, Y. Li, C.M. Devlin, D. Zhang, H.P. Harding, M. Sweeney, J.X. Rong, G. Kuriakose, E.A. Fisher, A.R. Marks, D. Ron, I. Tabas, The endoplasmic reticulum is the site of cholesterol-induced cytotoxicity in macrophages, Nat. Cell Biol. 5 (September (9)) (2003) 781–792.

[15] X. Kedi, Y. Ming, W. Yongping, Y. Yi, Z. Xiaoxiang, Free cholesterol overloading induced smooth muscle cells death and activated both ER- and mitochondrial-dependent death pathway, Atherosclerosis 207 (November (1)) (2009) 123–130.

[16] S.1 Rai, D.L. Hare, A. Zulli, A physiologically relevant atherogenic diet causes severe endothelial dysfunction within 4 weeks in rabbit, Int. J. Exp. Pathol. 90 (December (6)) (2009) 598–604, http://dx.doi.org/10.1111/j.1365-2613.2009.00668.x, Epub 2009 Sep 15.

[17] O.A. Rangel-Zuñiga, C. Haro, P. Perez-Martinez, J. Delgado-Lista, C. Marin, G.M. Quintana-Navarro, F.J. Tinahones, M.M. Malagón, F. Lopez-Segura, J. López-Miranda, F. Perez-Jimenez, A. Camargo, Effect of frying oils on the postprandial endoplasmic reticulum stress in obese people, Mol. Nutr. Food Res. 58 (November (11)) (2014) 2239–2242.

[18] D. Eberlé, B. Hegarty, P. Bossard, P. Ferré, F. Foufelle, SREBP transcription factors: master regulators of lipid homeostasis, Biochimie 86 (November (11)) (2004) 839–848.

[19] S.M. Colgan, D. Tang, G.H. Werstuck, R.C. Austin, Endoplasmic reticulum stress causes the activation of sterol regulatory element binding protein-2, Int. J. Biochem. Cell Biol. 39 (10) (2007) 1843–1851, Epub 2007 May 16.

[20] J. Han, R.J. Kaufman, The role of ER stress in lipid metabolism and lipotoxicity, J. Lipid Res. 57 (August (8)) (2016) 1329–1338, http://dx.doi.org/10.1194/jlr.R067595, Epub 2016 May 4.

[21] J. Ye, R.B. Rawson, R. Komuro, X. Chen, U.P. Davé, R. Prywes, M.S. Brown, J.L. Goldstein, ER stress induces cleavage of membrane-bound ATF6 by the same proteases that process SREBPs, Mol. Cell 6 (December (6)) (2000) 1355–1364.

[22] P. Lebeau, J.H. Byun, T. Yousof, R.C. Austin, Pharmacologic inhibition of S1P attenuates ATF6 expression, causes ER stress and contributes to apoptotic cell death, Toxicol. Appl. Pharmacol. 349 (June) (2018) 1–7, http://dx.doi.org/10.1016/j.taap.2018.04.020, Epub 2018 Apr 22.

[23] Tae-I, Jeon Seung-Soon Im, Dong-Ju Shin, F. Timothy, Osborne SREBP-1 Regulates UPR Signaling Biochemistry/Molecular Biology, 2011, http://dx.doi.org/10.1096/fasebj.25.1_supplement.741.2, 1 Apr 2011.

[24] K. Nemoto, A. Ikeda, S. Ito, M. Miyata, C. Yoshida, M. Degawa, Comparison of constitutive gene expression levels of hepatic cholesterol biosynthetic enzymes between Wistar-Kyoto and stroke-prone spontaneously hypertensive rats, Biol. Pharm. Bull. 36 (7) (2013) 1216–1220, Epub 2013 Apr 13.

[25] M. Pravenec, L. Kazdova, V. Landa, V. Zidek, P. Mlejnek, M. Simakova, P. Jansa, J. Forejt, V. Kren, D. Krenova, N. Qi, J.M. Wang, D. Chan, T.J. Aitman, T.W. Kurtz, Identification of mutated Srebf1 as a QTL influencing risk for hepatic steatosis in the spontaneously hypertensive rat, Hypertension 51 (January (1)) (2008) 148–153, Epub 2007 Dec 10.

[26] P. Pacher, T. Nagayama, P. Mukhopadhyay, S. Bátkai, D.A. Kass, Measurement of cardiac function using pressure-volume conductance catheter technique in mice and rats, Nat. Protoc. 3 (9) (2008) 1422–1434.

[27] J.C. Ikewuchi, E.N. Onyeike, A.A. Uwakwe, C.C. Ikewuchi, Effect of aqueous extract of the leaves of Acalypha wilkesiana 'Godseffiana' muell arg (Euphorbiaceae) on the hematology, plasma biochemistry and ocular indices of oxidative stress in alloxan induced diabetic rats, J. Ethnopharmacol. 137 (No. 3) (2011) 1415–1424.

[28] L.V. Tumanovs'ka, V.S. Nahibin, Dosenko VIe, O.O. Moĭbenko, Ultrastructural changes in isolated cardiomyocytes in modeling of endoplasmic reticulum stress, FiziolZh 54 (3) (2008) 10–21.

[29] A.H. Schönthal, Endoplasmic reticulum stress: its role in diseaseand novelprospects for therapy, Scientifica (Cairo) 2012 (2012) 857516.

[30] U.1 Ahmed, T.G. Redgrave, P.S. Oates, Effect of dietary fat to produce non-alcoholic fatty liver in the rat, J. Gastroenterol. Hepatol. 24 (August (8)) (2009) 1463–1471.

[31] N. Wu, X. Zhang, P. Jia, D. Jia, Hypercholesterolemia aggravates myocardial ischemia reperfusion injury via activating endoplasmic reticulum stress-mediated apoptosis, Exp. Mol. Pathol. 99 (December (3)) (2015) 449–454.

[32] M.A. Anwar, J. Shalhoub, C.S. Lim, M.S. Gohel, A.H. Davies, The effect of pressure-induced mechanical stretch on vascular wall differential gene expression, J. Vasc. Res. 49 (6) (2012) 463–478.

[33] J.H. Lin, H. Li, D. Yasumura, H.R. Cohen, C. Zhang, B. Panning, K.M. Shokat, M.M. Lavail, P. Walter, IRE1 signaling affects cell fate during the unfolded protein response, Science 318 (November (5852)) (2007) 944–949.

[34] X.F. Leong, C.Y. Ng, K. Jaarin, Animal models in cardiovascular research: hypertension and atherosclerosis, Biomed Res. Int. 2015 (2015) 528757, http://dx.doi.org/10.1155/2015/528757, Epub 2015 May 3.

[35] S.H. Quarfordt, B. Landis, G. Cucchiaro, Y. Yamaguchi, B. Oswald, Plasma cholesterol transport in anhepatic rats, J. Clin. Invest. 89 (5) (1992) 1564–1570.

[36] S.K. Choi, M. Lim, S.H. Byeon, Y.H. Lee, Inhibition of endoplasmic reticulum stress improves coronary artery function in the spontaneously hypertensive rats, Sci. Rep. 6 (August) (2016) 31925, http://dx.doi.org/10.1038/srep31925.

[37] J. Li, J.J. Wang, S.X. Zhang, Preconditioning with endoplasmic reticulum stress mitigates retinal endothelial inflammation via activation of X-box binding protein 1, J. Biol. Chem. 286 (February (6)) (2011) 4912–4921.

[38] Y. Ge, G. Li, B. Liu, H. Guo, D. Wang, Q. Jie, W. Che, L. Hou, Y. Wei, The protective effect of Lacidipine on myocardial remodeling is mediated by the suppression in expression of GPR78 and CHOP in rats, Evid. Complement. Alternat. Med. 2015 (2015), 945076.

[39] M. Sanchez-Alvarez, F. Finger, M. Arias-Garcia Mdel, V. Bousgouni, P. Pascual-Vargas, C. Bakal, Signaling networks converge on TORC1-SREBP activity to promote endoplasmic reticulum homeostasis, PLoS One 9 (July (7)) (2014), e101164.

[40] Y. Sun, T. Zhang, L. Li, J. Wang, Induction of apoptosis by hypertension via endoplasmic reticulum stress, Kidney Blood Press. Res. 40 (1) (2015) 41–51.